Analyzing the effects of central angle and applied voltage on the critical buckling temperature of a 2D-PFGM open cylindrical shell by GDQ method

Farhad Moradi [1], Saeed Jafari Mehrabadi [2], Mohammadreza Darmanaki Farahani [3]

[1] Department of Mechanical Engineering, Islamic Azad university, Arak Branch, Iran

[2] Department of Mechanical Engineering, Islamic Azad university, Arak Branch, Iran

[3] Department of Mechanical Engineering, Islamic Azad university, Central Tehran Branch, Iran

Abstract

In this paper, it is aimed to analyze the effects of variation of central angle and applied voltage on the critical buckling temperature of a thin cylindrical panel made of piezo-magnetic two-dimensional functionally graded material (2D-PFGM) subjected to constant magnetic field. Material properties of the structure assumed varying by exponential functions of volume fraction in longitudinal and circumferential directions. In order to tackle the problem, equilibrium equations have been initially derived by considering first order shear deformation theory and nonlinear terms of strain-displacement relations. In the following, by making incremental changes to the displacement components, calculating resultant forces and moments, and using Lagrang equations on the second functional variation of potential energy, the stability equations of the panel have been derived. After solving the mentioned equations by applying generalized differential quadrature method based on the simply supported boundary conditions, critical buckling temperature has been determined. Results from these formulas are discussed and compared with those obtained by other authors. At the end, effects of applied voltage to the external surface and central angel of the panel on the critical buckling temperature have been analyzed.

Keywords: *"Piezo-Magnetic"-"2D-PFGM"-"Thermal buckling"-"GDQ method"-"Thin cylindrical panel".*

1. Introduction

Circular cylindrical shells and panels have found many applications in engineering structures. Consequently, mechanical and thermal buckling of these structures has been extensively studied. In addition, since the last decade, due to the increasing demands for high heat-resistant, lightweight structures, interest in functionally graded structures, especially FG cylindrical shells, has drastically increased. Functionally graded materials (FGMs) are a new generation of composite materials, in which the volume fraction of two or more materials varied as a function of the position along a certain dimension [1].

Knowledge and findings about the behavior of magneto-electro-elastic structures has gained more importance recently as these smart structures have special ability for converting energy from one form to another (among magnetic, electric, and mechanical energy). The magneto-electric coupling effect in composite materials consisting a piezo-electric and a piezo-magnetic phase has recently attracted much more attention owing to the extensive applications for broadband magnetic field probes, electric packaging, acoustic, hydrophones, medical ultrasonic imaging, sensors, and actuators [2, 3, 4, and 5]. These composites are usually considered as smart or intelligent materials. The analytical modeling of such composites provides valuable opportunities for studying the effect of controlling and altering the response of composite structures made of these materials. Pan [6] derived exact solution for a simply supported and multilayered plate made of anisotropic piezoelectric and piezomagnetic materials under a static and mechanical load. Pan and Heyliger [7] solved a vibration problem of these materials. Bhangale and Ganensan [8] presented a static analysis for functionally graded; anisotropic, linear magneto-electro-elastic plates by a semi-analytical finite element method. Piezoelectric and piezomagnetic composites depict a coupling effect of electric and magnetic fields.

Many researchers have investigated buckling analysis of various structures since the last 10 years. Shen [9, 10] presented a post buckling analysis for nanocomposite cylindrical shells reinforced by single-walled carbon nanotubes subject to axial compression and lateral or hydrostatic pressure in thermal environments. Thermal buckling analysis of moderately thick composite cylindrical shells under asymmetric thermal loading presented by Darvizeh et al. [11]. Shariyat [12] studied dynamic buckling of imperfect laminated plates with piezoelectric sensors and actuators subjected to thermo-electro-mechanical loadings, considering the temperature-dependency of material properties using a finite element method based on a higher-order shear deformation theory. Eslami et al. [13] investigated the thermoelastic buckling of thin cylindrical shells based on improved stability equations and Sanders assumptions. An exact solution for classic

[1] M.S. graduated from university (corresponding author)
Email address: engmechmoradi@gmail.com

[2] Professor of Arak Azad University

[3] B.S. graduated from university

coupled magneto-thermo-elasticity in cylindrical coordinates is developed by Jabbari et al. [14]. Long and Xuewu [15] presented buckling and vibration analysis for a functionally graded magneto-electro-thermo-elastic (FGMETE) circular cylindrical shell. In this paper, the influences of various kinds of external loads, such as axial force, different temperatures, surface electric and magnetic voltage, on the buckling response of the shell investigated. Aboudi [16] and Lee [17] developed a micromechanics method for the prediction of the effective behavior of fully coupled electro-magneto-thermo-elastic Multiphase composites. Biju et al. [18] studied the behavior of multiphase magneto-electro-elastic sensors under harmonic mechanical loading using finite element method. Micromechanical modeling and behavior analysis of smart magneto-electro-elastic materials using finite element method presented by Tian and Yu [19] and Kondaiah et al. [20]. Malekzadeh and Heydarpour [21] presented a transient thermo-elastic analysis of FGM cylindrical shells under moving boundary pressure and heat flux. In order to benefit from the high accuracy and low computational efforts of the DQM in conjunction with the effectiveness of the FEM in general geometry, loading and systematic boundary treatment, a combination of these methods was employed to discretize the governing equations in the spatial domain.

In FGMs, material properties are usually assumed varying in one direction. If the FGM has two-dimensional dependent material properties, more effective material can be obtained. Based on this assumption, two-dimensional functionally graded materials with bi-directional dependent properties have been introduced. Jafari Mehrabadi and Sobhani [22] studied the thermoelastic analysis of a 2D functionally graded open cylindrical shell based on third-order shear deformation theory of Reddy. They proposed a 2D power-law distribution for volume fractions of 2D FGM. The governing equations and associated boundary conditions were derived using the Hamilton's principle, and discretized by applying GDQM.

Obtaining the exact solution for governing equations becomes more complicated because properties of the 2D FGM are functions of positions. Owing to that, various methods including finite element method (FEM), finite difference method (FDM), boundary element method (BEM), and differential quadrature method (DQM) can be employed to analyze thermal buckling and stability of structures. DQM introduced by Bellman and Casti [23] for the first time. By utilizing this method, partial differential governing equations converted to linear algebraic equations. The improved version of DQM called generalized differential quadrature method (GDQM) introduced by Shu [24]. In this study, GDQM approach is used to discretize the governing equations of 2D-PFGM open cylindrical shell as an efficient and accurate numerical method [25–27].

The present work focuses on Magneto-Thermo-Elastic buckling analysis of a 2D PFGM open cylindrical shell. The material properties (Young's modulus and density) are assumed to vary continuously through longitudinal and circumferential directions according to the rule of mixtures. The volume fraction is estimated through a volume fraction power-law. Nonlinear strain-displacement relations in cylindrical coordinates are considered. The total potential energy function for magneto-thermo-elastic loading present. Euler equations applied to the function of potential energy, and nonlinear stability equations of shells are obtained. The nonlinear stability equations of 2D PFGM open cylindrical shells for simply supported boundary conditions are derived using the variation formulation, and discretized by means of the generalized differential quadrature method (GDQM) to obtain critical temperature difference. Results are presented to analyze the effects of applied voltage to the external surface and central angle of the panel.

2. Modeling and Formulation

Consider a piezo-magnetic 2D-FG open cylindrical shell, in which α and R are angle and radius, respectively. The reference surface of the panel considered at its middle. Open cylindrical shell is subjected to a uniform magnetic field in x, θ and z direction.

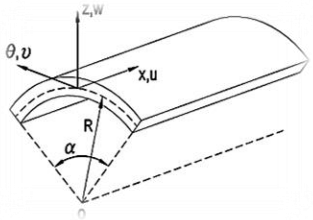

Fig. 1: The schematic of an open cylindrical shell with the curvilinear coordinate system.

The 2D-FGM open cylindrical shell is made by continuous gradation of four materials, two ceramics and two alloy metals. Volume fractions of the constituents vary in the longitudinal and circumferential directions as shown in Fig. 2. The volume fraction of the first ceramic material is changed from 1 at $(\mathrm{x}, \theta) = (0, \alpha)$ to zero at $(\mathrm{x}, \theta) = (L, \alpha)$ by a power-law function. In addition, this volume fraction is changed continuously from 1 at $(\mathrm{x}, \theta) = (0,0)$ to zero at $(\mathrm{x}, \theta) = (0, \alpha)$. The volume fractions of the other materials change in a similar way in two directions. The constituents volume fraction are estimated as [28].

$$V_{m1}(x,\theta) = \left[1 - \left(\frac{\theta}{\alpha}\right)^{n_\theta}\right]\left[1 - \left(\frac{x}{L}\right)^{n_x}\right]$$
$$V_{m2}(x,\theta) = \left[1 - \left(\frac{\theta}{\alpha}\right)^{n_\theta}\right]\left[\left(\frac{x}{L}\right)^{n_x}\right]$$
$$V_{c1}(x,\theta) = \left[1 - \left(\frac{x}{L}\right)^{n_x}\right]\left[\left(\frac{\theta}{\alpha}\right)^{n_\theta}\right]$$
$$V_{c2}(x,\theta) = \left[\left(\frac{x}{L}\right)^{n_x}\right]\left[\left(\frac{\theta}{\alpha}\right)^{n_\theta}\right] \quad (1)$$

that $V_{mi}(i = 1,2)$ and $V_{ci}(i = 1,2)$ are volume fractions of metals and ceramics, respectively. Moreover, n_x and

n_θ are the constant exponent of volume fraction power-law and $n_x, n_\theta \geq 0$.

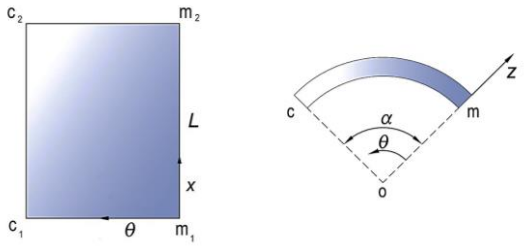

Fig. 2: Top and side view of 2D FGM open cylindrical shell.

The effective material properties of the open cylindrical shell can expressed as [28]

$$P(\theta,x) = P_{m1}V_{m1} + P_{m2}V_{m2} + P_{c1}V_{c1} + P_{c2}V_{c2} \qquad (2)$$

that $P(\theta,x)$ is the material property of the FGM shell. Moreover, $P_{mi}(i = 1,2)$ and $P_{ci}(i = 1,2)$ are material properties of metals and ceramics, respectively.

Reddy's first order shear deformation description of the displacement field [29]

$$\begin{aligned} u(x,\theta,z) &= u_0(x,\theta) + z\psi(x,\theta) \\ v(x,\theta,z) &= v_0(x,\theta) + z\varphi(x,\theta) \\ w(x,\theta,z) &= w_0(x,\theta) \end{aligned} \qquad (3)$$

The displacement components along x, θ and z direction are denoted by $u(x,\theta,z)$, $v(x,\theta,z)$ and $w(x,\theta,z)$, respectively. $u_0(x,\theta)$, $v_0(x,\theta)$ and $w_0(x,\theta)$ are displacement components in mid-surface. $\varphi(x,\theta)$, and $\psi(x,\theta)$ denote rotations about x and θ axes, respectively.

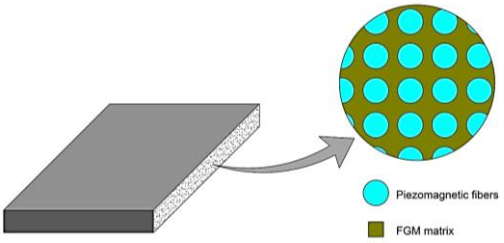

Fig. 3: Multi-phase magneto-elastic composite.

The nonlinear strain–displacement relations are as [29]

$$\begin{aligned} \varepsilon_{xx} &= u_{,x} + \frac{1}{2}w_{,x}^2 \\ \varepsilon_{\theta\theta} &= \frac{1}{R}(w + v_{,\theta}) + \frac{1}{2R^2}w_{,\theta}^2 \\ \varepsilon_{zz} &= 0 \\ \gamma_{x\theta} &= \frac{1}{R}u_{,\theta} + v_{,x} + \frac{1}{R}w_{,x}w_{,\theta} \\ \gamma_{xz} &= w_{,x} + u_{,z} \\ \gamma_{\theta z} &= \frac{1}{R}w_{,\theta} + v_{,z} \end{aligned} \qquad (4)$$

Substituting Eq. (3) in Eq. (4)

$$\begin{Bmatrix} \varepsilon_{xx} \\ \varepsilon_{\theta\theta} \\ \gamma_{x\theta} \\ \gamma_{xz} \\ \gamma_{\theta z} \end{Bmatrix} = \begin{Bmatrix} \varepsilon_{xxm} \\ \varepsilon_{\theta\theta m} \\ \gamma_{x\theta m} \\ \gamma_{xzm} \\ \gamma_{\theta zm} \end{Bmatrix} + z\begin{Bmatrix} k_x \\ k_\theta \\ 2k_{x\theta} \\ 0 \\ 0 \end{Bmatrix} \qquad (5)$$

$$\begin{Bmatrix} \varepsilon_{xxm} \\ \varepsilon_{\theta\theta m} \\ \gamma_{x\theta m} \\ \gamma_{xzm} \\ \gamma_{\theta zm} \end{Bmatrix} = \begin{Bmatrix} u_{0,x} + \frac{1}{2}w_{0,x}^2 \\ \frac{1}{R}(w_0 + v_{0,\theta}) + \frac{1}{2R^2}w_{0,\theta}^2 \\ \frac{1}{R}u_{0,\theta} + v_{0,x} + \frac{1}{R}w_{0,x}w_{0,\theta} \\ w_{0,x} + \psi \\ \frac{1}{R}w_{0,\theta} + \varphi \end{Bmatrix}$$

$$\begin{Bmatrix} k_x \\ k_\theta \\ k_{x\theta} \end{Bmatrix} = \begin{Bmatrix} \psi_{,x} \\ \frac{1}{R}\varphi_{,\theta} \\ \frac{1}{2}\left(\frac{1}{R}\psi_{,\theta} + \varphi_{,x}\right) \end{Bmatrix} \qquad (6)$$

The index m indicates mid-surface strains. k_x, k_θ and $k_{x\theta}$ are curvatures. The distribution of magnetic potential along the thickness direction is approximated as below

$$\eta_H(x,\theta,z) = \frac{2z}{h}V_H(x,\theta) \qquad (7)$$

where V_H is the external surface magnetic voltage of the open cylindrical shell. To Study the influence of uniform magnetic field on critical temperature difference of the cylindrical panel, a composite material with piezo-magnetic fibers is considered. The constitutive relations for 2D PFGM open cylindrical shell [15]

$$\begin{Bmatrix} \sigma_{xx} \\ \sigma_{\theta\theta} \\ \tau_{\theta z} \\ \tau_{xz} \\ \tau_{x\theta} \end{Bmatrix} = \begin{bmatrix} Q_{11} & Q_{12} & 0 & 0 & 0 \\ Q_{21} & Q_{22} & 0 & 0 & 0 \\ 0 & 0 & Q_{44} & 0 & 0 \\ 0 & 0 & 0 & Q_{55} & 0 \\ 0 & 0 & 0 & 0 & Q_{66} \end{bmatrix} \begin{Bmatrix} \varepsilon_{xx} - \alpha(x,\theta)T(z) \\ \varepsilon_{\theta\theta} - \alpha(x,\theta)T(z) \\ \gamma_{\theta z} \\ \gamma_{xz} \\ \gamma_{x\theta} \end{Bmatrix} - \begin{bmatrix} 0 & 0 & q_{31} \\ 0 & 0 & q_{32} \\ 0 & q_{24} & 0 \\ q_{15} & 0 & 0 \\ 0 & 0 & 0 \end{bmatrix} \begin{Bmatrix} H_{xx} \\ H_{\theta\theta} \\ H_{zz} \end{Bmatrix}$$

$$\begin{Bmatrix} B_{xx} \\ B_{\theta\theta} \\ B_{zz} \end{Bmatrix} = \begin{bmatrix} 0 & 0 & 0 & q_{15} & 0 \\ 0 & 0 & q_{24} & 0 & 0 \\ q_{31} & q_{32} & 0 & 0 & 0 \end{bmatrix} \begin{Bmatrix} \varepsilon_{xx} \\ \varepsilon_{\theta\theta} \\ \gamma_{\theta z} \\ \gamma_{xz} \\ \gamma_{x\theta} \end{Bmatrix} + \begin{bmatrix} \mu_{11} & 0 & 0 \\ 0 & \mu_{22} & 0 \\ 0 & 0 & \mu_{33} \end{bmatrix} \begin{Bmatrix} H_{xx} \\ H_{\theta\theta} \\ H_{zz} \end{Bmatrix} \qquad (8)$$

where σ_{ii} is normal stress components, τ_{ij} are shear stress components, ε_{ii} is normal strain components, γ_{ij} is shear strain, B_{ii} is magnetic induction, μ_{ii} is magnetic constant, q_{ij} is piezo-magnetic constant, $\alpha(x,\theta)$ is thermal expansion coefficient, H_{ii} is magnetic field component and Q_{ij} is constant, where defined as follow [15, 29]

$$\begin{aligned} H_{\theta\theta} &= -\frac{1}{R+z}\frac{\partial \eta_H}{\partial \theta} = -\frac{2z}{h(R+z)}V_{H,\theta} \\ H_{zz} &= -\frac{\partial \eta_H}{\partial z} = -\frac{2}{h}V_H \\ H_{xx} &= -\frac{\partial \eta_H}{\partial x} = -\frac{2z}{h}V_{H,x} \\ Q_{11} &= Q_{22} = \frac{E(x,\theta)}{1-\nu^2} \\ Q_{12} &= Q_{21} = \frac{\nu E(x,\theta)}{1-\nu^2} \\ Q_{44} &= Q_{55} = Q_{66} = \frac{E(x,\theta)}{2(1+\nu)} \end{aligned} \qquad (9)$$

It is assumed that magnetic field has to satisfy the following equation [30]

$$\vec{\nabla}.\vec{B} = 0 \tag{10}$$

Substituting Eqs. (5, 7 and 9) in Eq. (8) lead to

$$\begin{aligned}
\sigma_{xx} &= Q_{11}\varepsilon_{xxm} + Q_{12}\varepsilon_{\theta\theta m} + z(Q_{11}k_x + Q_{12}k_\theta) - \\
&\quad Q_{11}\alpha(x,\theta)T(z) - Q_{12}\alpha(x,\theta)T(z) + \frac{2q_{31}}{h}V_H \\
\sigma_{\theta\theta} &= Q_{12}\varepsilon_{xxm} + Q_{22}\varepsilon_{\theta\theta m} + z(Q_{12}k_x + Q_{22}k_\theta) - \\
&\quad Q_{12}\alpha(x,\theta)T(z) - Q_{22}\alpha(x,\theta)T(z) + \frac{2\mu_{33}}{h}\frac{2q_{32}}{h}V_H \\
\tau_{\theta z} &= Q_{44}\gamma_{\theta zm} + \frac{2zq_{24}}{h(R+z)}V_{H,\theta} \\
\tau_{x\theta} &= Q_{66}\gamma_{x\theta m} + 2zQ_{66}k_{x\theta} \\
B_{xx} &= q_{15}\gamma_{xzm} - \frac{2z\mu_{11}}{h}V_{H,x} \\
B_{\theta\theta} &= q_{24}\gamma_{\theta zm} - \frac{2z\mu_{22}}{h(R+z)}V_{H,\theta} \\
B_{zz} &= [q_{31}\varepsilon_{xxm} + q_{32}\varepsilon_{\theta\theta m}] + z[q_{31}k_x + q_{32}k_\theta] \\
&\quad - \frac{2\mu_{33}}{h}V_H
\end{aligned} \tag{11}$$

The total potential energy of the open cylindrical shell written as [31]

$$V = U + \Omega \tag{12}$$

Where U and Ω are strain energy and external work, respectively, and are as follow [15, 29]

$$\begin{aligned}
U &= \frac{1}{2}\int\{\sigma_{xx}\varepsilon_{xx} + \sigma_{\theta\theta}\varepsilon_{\theta\theta} + \tau_{x\theta}\gamma_{x\theta} + \tau_{xz}\gamma_{xz} + \tau_{z\theta}\gamma_{z\theta} \\
&\quad -\sigma_{xx}\alpha(x,\theta)T(z) - \sigma_{\theta\theta}\alpha(x,\theta)T(z) + B_{xx}H_{xx} \\
&\quad +B_{\theta\theta}H_{\theta\theta} + B_{zz}H_{zz}\}dV \\
\Omega &= \frac{1}{2}\int(N_x^H - N_x^T)\left(w_{,x}^2 + v_{,x}^2\right)dA
\end{aligned} \tag{13}$$

N_x^H and N_x^T are magnetic and thermal loads and are defined as follow [15]

$$\begin{aligned}
N_x^H &= V_H\int_{-\frac{h}{2}}^{\frac{h}{2}}\frac{2q_{31}}{h}dz \\
N_x^T &= \int_{-\frac{h}{2}}^{\frac{h}{2}}\{Q_{11}\alpha(x,\theta) + Q_{12}\alpha(x,\theta)\}T(z)dz
\end{aligned} \tag{14}$$

Force and moment resultants are defined as follow [29]

$$\begin{aligned}
(N_i, M_i) &= \int_{-\frac{h}{2}}^{\frac{h}{2}}\sigma_i(1,z)dz \qquad i = x,\theta \\
Q_i &= \int_{-\frac{h}{2}}^{\frac{h}{2}}\sigma_{iz}dz \qquad i = x,\theta
\end{aligned} \tag{15}$$

In addition, the following coefficients are defined as

$$\begin{aligned}
A_{11},A_{12},A_{22},A_{44},A_{55} &= \int_{-\frac{h}{2}}^{\frac{h}{2}}\{Q_{11},Q_{12},Q_{22},Q_{44},Q_{55}\}dz \\
B_{11},B_{12},B_{22},B_{66} &= \int_{-\frac{h}{2}}^{\frac{h}{2}}z\{Q_{11},Q_{12},Q_{22},2Q_{66}\}dz \\
C_{11},C_{12},C_{22} &= \int_{-\frac{h}{2}}^{\frac{h}{2}}\{Q_{11},Q_{12},Q_{22}\}\alpha(x,\theta)T(z)dz \\
D_{11},D_{12},D_{22},D_{66} &= \int_{-\frac{h}{2}}^{\frac{h}{2}}z^2\{Q_{11},Q_{12},Q_{22},2Q_{66}\}dz \\
T_{11},T_{12},T_{22} &= \int_{-\frac{h}{2}}^{\frac{h}{2}}z\{Q_{11},Q_{12},Q_{22}\}\alpha(x,\theta)T(z)dz \\
P_{11},P_{12},P_{22} &= \int_{-\frac{h}{2}}^{\frac{h}{2}}\{Q_{11},Q_{12},Q_{22}\}\alpha^2(x,\theta)T^2(z)dz \\
G_1,G_2 &= \int_{-\frac{h}{2}}^{\frac{h}{2}}\frac{1}{h}\{q_{31},q_{32}\}\alpha(x,\theta)T(z)dz \\
S_1,S_2 &= \int_{-\frac{h}{2}}^{\frac{h}{2}}\frac{1}{h}\{q_{31},q_{32}\}dz \\
m_{11},m_{22},m_{33} &= \int_{-\frac{h}{2}}^{\frac{h}{2}}\frac{4}{h^2}\left\{z^2\mu_{11},\frac{z^2\mu_{22}}{(R+z)^2},\mu_{33}\right\}dz \\
n_1,n_2,I_1,I_2 &= \int_{-\frac{h}{2}}^{\frac{h}{2}}\frac{z}{h}\left\{q_{31},q_{32},q_{15},\frac{q_{24}}{R+z}\right\}dz \\
G_1 + G_2 &= G_3
\end{aligned} \tag{16}$$

Substituting Eqs. (11, 13, 14 and 15) in Eq. (12) and applying Euler equations equilibrium equations for the shell obtained as below

$$\begin{aligned}
&RN_{xx,x} + N_{x\theta,\theta} - 2S_1V_{H,x} = 0 \\
&RN_{x\theta,x} + N_{\theta\theta,\theta} + (N_x^H - N_x^T)v_{0,xx} + 2S_1V_{H,x}v_{0,x} \\
&-2S_1V_{H,\theta} = 0 \\
&N_{\theta\theta} + RN_x^Tw_{0,xx} - 2S_1V_{H,x}w_{0,x} - RN_{xx}w_{0,xx} - RQ_{x,x} \\
&-2N_{x\theta}w_{0,x\theta} - Q_{\theta,\theta} - \frac{1}{R}w_{0,\theta\theta}N_{\theta\theta} + \frac{2}{R}S_2w_{0,\theta\theta}V_H \\
&-\frac{1}{R}w_{0,\theta}\left[(N_x^H - N_x^T)v_{0,xx} - 2S_1V_{H,x}v_{0,x}\right] \\
&+2RI_1V_{H,xx} + 2I_2V_{H,\theta\theta}\ 2S_2V_H = 0 \\
&RQ_x - RM_{xx,x} - M_{x\theta,\theta} + 2R(n_1 - I_1)V_{H,x} = 0 \\
&RQ_\theta - RM_{x\theta,x} - M_{\theta\theta,\theta} + 2(n_2 - RI_2)V_{H,\theta} = 0 \\
&RS_1\left(w_{0,x}^2 + v_{0,x}^2\right) + Rm_{33}V_H - RG_3 - Rm_1V_{H,xx} \\
&-Rm_{22}V_{H,\theta\theta} = 0
\end{aligned} \tag{17}$$

Stability equations for 2D FGM thin cylindrical panel can be obtained by applying variation method to total potential energy of the structure. Applying first variation δV leads to equilibrium equations and second variation δ^2V to write stability equations. Critical buckling temperature is a temperature that the structure is not stable, i.e. is the minimum temperature, the value of second variation of potential energy larger than zero. To obtain buckling temperature δ^2V equal to zero. Applying equations functional of second variation of potential energy, the equations are as follow

$$\begin{aligned}
&RN_{xx1,x} + N_{x\theta1,\theta} = 0 \\
&RN_{x\theta1,x} + N_{\theta\theta1,\theta} + R(N_x^H - N_x^T)v_{1,xx} + 2RS_1v_{H,x}v_{1,x} \\
&= 0 \\
&N_{\theta\theta1} - Rw_{1,xx}N_{xx0} - 2w_{1,x\theta}N_{x\theta0} - RQ_{x1,x} - Q_{\theta1,\theta} \\
&-\frac{1}{R}w_{1,\theta\theta}N_{\theta\theta0} + \frac{2}{R}S_2w_{1,\theta\theta}v_H - 2S_1w_{1,x}v_x \\
&+\frac{1}{R}w_{1,\theta}\left(2S_1v_{H,x}v_{0,x} + (N_x^H - N_x^T)v_{0,xx}\right) = 0 \\
&RQ_{x1} - RM_{xx1,x} - M_{x\theta1,\theta} = 0 \\
&RQ_{\theta1} - RM_{x\theta1,x} - M_{\theta\theta1,\theta} = 0
\end{aligned} \tag{18}$$

The terms by subscript '0,' show equilibrium state and terms by subscript '1' refer to stability situation. Substituting Eq. (6) in Eq. (18) leads to stability equations in terms of displacement components is obtained. The critical temperature difference is defined as: $\Delta T_{cr} = T_f - T_i$.

$$N_{x\theta 0} = N_{\theta\theta 0} = 0$$

$$N_{xx0} = N_x^H - N_x^T = 2S_1V_H - (C_{11} + c_{12}) = 2S_1V_H - \beta\Delta T$$

$$\beta = \int_{\frac{-h}{2}}^{\frac{h}{2}} \{Q_{11} + Q_{12}\}\alpha(x,\theta)dz \tag{19}$$

Solving the stability equations, simply support boundary conditions considered for edges $x = 0, L$, $\theta = 0, \alpha$ of the open cylindrical shell and formulated as

$$v_1 = w_1 = \varphi_1 = M_{xx1} = N_{xx1} = 0 \quad at\ x = 0, L$$
$$u_1 = w_1 = \psi_1 = M_{\theta\theta 1} = N_{\theta\theta 1} = 0 \quad at\ \theta = 0, \alpha \tag{20}$$

By substituting Eqs. (19) and (20) into Eq. (18), stability equations can be written as

$$RN_{xx1,x} + N_{x\theta 1,\theta} = 0$$
$$RN_{x\theta 1,x} + N_{\theta\theta 1,\theta} + R(N_x^H - N_x^T)V_{1,xx} = 0$$
$$N_{\theta\theta 1} - RW_{1,xx}(N_x^H - N_x^T)Q_{x1,x}Q_{\theta 1,\theta} + \frac{2}{R}S_2W_{1,\theta\theta}V_H = 0$$
$$RQ_{x1} - R\,M_{xx1,x} - M_{x\theta 1,\theta} = 0$$
$$RQ_{\theta 1} - R\,M_{x\theta 1,x} - M_{\theta\theta 1,\theta} = 0 \tag{21}$$

Force and moment resultants on the close vicinity of equilibrium according to Eq. (15) are defined as follow

$$N_{xx1} = A_{11}U_{1,x} + \frac{A_{12}}{R}(W_1 + V_{1,\theta}) + B_{11}\psi_{1,x} + \frac{B_{12}}{R}\varphi_{1,\theta}$$
$$N_{\theta\theta 1} = A_{12}U_{1,x} + \frac{A_{22}}{R}V_{1,\theta} + \frac{A_{22}}{R}W_1 + B_{12}\psi_{1,x} + \frac{B_{22}}{R}\varphi_{1,\theta}$$
$$N_{x\theta 1} = A_{66}\left(V_{1,x} + \frac{1}{R}U_{1,\theta}\right) + \frac{B_{66}}{2}\left(\varphi_{1,x} + \frac{1}{R}\psi_{1,\theta}\right)$$
$$M_{xx1} = B_{11}U_{1,x} + \frac{B_{12}}{R}(W_1 + V_{1,\theta}) + D_{11}\psi_{1,x} + \frac{D_{12}}{R}\varphi_{1,\theta}$$
$$M_{\theta\theta 1} = B_{12}U_{1,x} + \frac{B_{22}}{R}V_{1,\theta} + \frac{A_{22}}{R}W_1 + D_{12}\psi_{1,x} + \frac{D_{22}}{R}\varphi_{1,\theta}$$
$$M_{xx1} = \frac{1}{2}\left\{B_{66}\left(V_{1,x} + \frac{1}{R}U_{1,\theta}\right) + \frac{D_{66}}{2}\left(\varphi_{1,x} + \frac{1}{R}\psi_{1,\theta}\right)\right\}$$
$$Q_{x1} = A_{55}(\psi_1 + W_{1,x})$$
$$Q_{\theta 1} = A_{44}\left(\varphi_1 + \frac{1}{R}W_{1,\theta}\right) \tag{22}$$

For simplify the coefficients in Eqs. (16), applying integrals, defined as follow

$$A_{12} = A_{21} = K_2(x,\theta)h \qquad S_1 = q_{31}$$
$$B_{11} = B_{12} = B_{22} = B_{66} = 0 \qquad S_2 = q_{32}$$
$$A_{44} = A_{55} = A_{66} = K_3(x,\theta)h \qquad K_1(x,\theta) = \frac{E(x,\theta)}{1-\upsilon^2}$$
$$A_{11} = A_{22} = K_1(x,\theta)h \qquad K_2(x,\theta) = \frac{\nu E(x,\theta)}{1-\upsilon^2}$$
$$D_{11} = D_{22} = K_1(x,\theta)\frac{h^3}{12} \qquad K_3(x,\theta) = \frac{E(x,\theta)}{2(1+\nu)}$$
$$D_{12} = D_{21} = K_2(x,\theta)\frac{h^3}{12}$$
$$D_{66} = K_3(x,\theta)\frac{h^3}{12}$$
$$N_x^H = 2q_{31}V_H$$
$$N_x^T = \big(K_1(x,\theta) + K_2(x,\theta)\big)\alpha(x,\theta)h\Delta T \tag{23}$$

3. Solution

According to generalized differential quadrature method, *m*th order derivative of the solution function with respect to a space variable *x*, θ at a given grid point *i* can be approximated as follow [33]

$$\frac{\partial^m f(x_i,\theta_j)}{\partial x^m} = \sum_{n=1}^{N_x} A_{in}^{(m)} f(x_n,\theta_j) \quad i = 1,2,.,N_x\ , j = 1,2,.,N_\theta$$
$$\frac{\partial^m f(x_i,\theta_j)}{\partial \theta^m} = \sum_{n=1}^{N_x} B_{jn}^{(m)} f(x_n,\theta_j) \quad \mathrm{i} = 1,2,.,N_x\ , j = 1,2,.,N_\theta \tag{24}$$

where $A_{ij}^{(m)}$ is weight coefficients in *x* direction, $B_{jn}^{(m)}$ is weight coefficients in θ direction, N_x and N_θ are the number of grid points in x, θ directions, respectively. The value of coefficients matrix is calculated according to the following equations [33, 34]

$$A_{ij}^{(1)} = \frac{M(x_i)}{(x_i - x_j)M(x_j)} \qquad For\ i \neq j$$
$$A_{ii}^{(1)} = -A_{ij}^{(1)}$$
$$M(x_i) \prod_{k=1,k\neq i}^{N} (x_i - x_k)$$
$$A_{ij}^{(2)} = 2A_{ij}^{(1)}\left[A_{ii}^{(1)} - \frac{1}{x_i - x_j}\right] \qquad For\ i \neq j$$
$$A_{ii}^{(2)} = -\sum_{j=1,i\neq j}^{N} A_{ij}^{(2)} \tag{25}$$

Substituting Eqs. (25, 26) in Eq. (24) leads to

$$R\frac{\partial K_1(x,\theta)}{\partial x}h\sum_{n=1}^{N_x} A_{in}^{(1)}u_{nj} + R\,K_1(x,\theta)h\sum_{n=1}^{N_x} A_{in}^{(2)}u_{nj}$$
$$+h\frac{\partial K_2(x,\theta)}{\partial x}\left(w_{ij} + \sum_{m=1}^{N_\theta} B_{jm}^{(1)}v_{im}\right) + hK_2(x,\theta)$$
$$\left(\sum_{n=1}^{N_x} A_{in}^{(1)}w_{nj} + \sum_{n=1}^{N_x}\sum_{m=1}^{N_\theta} A_{in}^{(1)}B_{jm}^{(1)}v_{nm}\right) + h\frac{\partial K_2(x,\theta)}{\partial \theta}$$
$$\left(\sum_{n=1}^{N_x} A_{in}^{(1)}v_{nj} + \frac{1}{R}\sum_{m=1}^{N_\theta} B_{jm}^{(1)}u_{im}\right) + hK_2(x,\theta)$$
$$\left(\sum_{n=1}^{N_x}\sum_{m=1}^{N_\theta} A_{in}^{(1)}B_{jm}^{(1)}v_{nm} + \frac{1}{R}\sum_{m=1}^{N_\theta} B_{jm}^{(1)}u_{im}\right) = 0$$
$$Rh\frac{\partial K_3(x,\theta)}{\partial x}\left(\sum_{n=1}^{N_x} A_{in}^{(1)}v_{nj} + \frac{1}{R}\sum_{m=1}^{N_\theta} B_{jm}^{(1)}u_{im}\right) + RhK_3(x,\theta)$$
$$\left(\sum_{n=1}^{N_x} A_{in}^{(2)}v_{nj} + \frac{1}{R}\sum_{n=1}^{N_x}\sum_{m=1}^{N_\theta} A_{in}^{(1)}B_{jm}^{(1)}u_{nm}\right) + h\frac{\partial K_2(x,\theta)}{\partial \theta}$$
$$\sum_{n=1}^{N_x} A_{in}^{(1)}u_{nj} + hK_2(x,\theta)\sum_{n=1}^{N_x}\sum_{m=1}^{N_\theta} A_{in}^{(1)}B_{jm}^{(1)}u_{nm} + \frac{h}{R}\frac{\partial K_2(x,\theta)}{\partial \theta}$$
$$\left(w_{ij} + \sum_{m=1}^{N_\theta} B_{jm}^{(1)}v_{im}\right) + +2Rq_{31}V_H\sum_{n=1}^{N_x} A_{in}^{(2)}v_{nj}$$
$$+\frac{h}{R}K_2(x,\theta)\left(\sum_{m=1}^{N_\theta} B_{jm}^{(1)}w_{im} + \sum_{m=1}^{N_\theta} B_{jm}^{(2)}v_{im}\right)$$
$$-R[K_1(x,\theta) + K_2(x,\theta)]\alpha(x,\theta)h\Delta T\sum_{n=1}^{N_x} A_{in}^{(2)}v_{nj} = 0$$

$$hK_2(x,\theta)\sum_{n=1}^{N_x}A_{in}^{(1)}u_{nj}+\frac{h}{R}K_1(x,\theta)\left(w_{ij}+\sum_{m=1}^{N_\theta}B_{jm}^{(1)}v_{im}\right)$$
$$+Rh\frac{\partial K_3(x,\theta)}{\partial x}\left(\psi_{ij}+\sum_{n=1}^{N_x}A_{in}^{(1)}w_{nj}\right)+RhK_3(x,\theta)$$
$$\left(\sum_{n=1}^{N_x}A_{in}^{(1)}\psi_{nj}+\sum_{n=1}^{N_x}A_{in}^{(2)}w_{nj}\right)+h\frac{\partial K_3(x,\theta)}{\partial\theta}$$
$$\left(\varphi_{ij}+\frac{1}{R}\sum_{m=1}^{N_\theta}B_{jm}^{(1)}w_{im}\right)+hK_3(x,\theta)$$
$$\left(\sum_{m=1}^{N_\theta}B_{jm}^{(1)}\varphi_{im}+\frac{1}{R}\sum_{m=1}^{N_\theta}B_{jm}^{(2)}w_{im}\right)+\frac{2}{R}q_{32}V_H\sum_{m=1}^{N_\theta}B_{jm}^{(2)}w_{im}$$
$$-2Rq_{31}V_H\sum_{n=1}^{N_x}A_{in}^{(2)}w_{nj}+R[K_1(x,\theta)+K_2(x,\theta)]\alpha(x,\theta)h\Delta T$$
$$\sum_{n=1}^{N_x}A_{in}^{(2)}w_{nj}=0$$
$$RhK_3(x,\theta)\left(\psi_{ij}+\sum_{n=1}^{N_x}A_{in}^{(1)}w_{nj}\right)-R\frac{h^3}{12}\frac{\partial K_1(x,\theta)}{\partial x}\sum_{n=1}^{N_x}A_{in}^{(1)}\psi_{nj}$$
$$-R\frac{h^3}{12}K_1(x,\theta)\sum_{n=1}^{N_x}A_{in}^{(2)}\psi_{nj}-\frac{h^3}{12}\frac{\partial K_1(x,\theta)}{\partial x}$$
$$-\frac{h^3}{12}K_2(x,\theta)\sum_{n=1}^{N_x}\sum_{m=1}^{N_\theta}A_{in}^{(1)}B_{jm}^{(1)}\varphi_{nm}$$
$$-\frac{h^3}{24}\frac{\partial K_3(x,\theta)}{\partial\theta}\left(\sum_{n=1}^{N_x}A_{in}^{(1)}\varphi_{nj}+\frac{1}{R}\sum_{m=1}^{N_\theta}B_{jm}^{(1)}\psi_{im}\right)$$
$$-\frac{h^3}{24}K_3(x,\theta)\left(\sum_{n=1}^{N_x}\sum_{m=1}^{N_\theta}A_{in}^{(1)}B_{jm}^{(1)}\varphi_{nm}+\frac{1}{R}\sum_{m=1}^{N_\theta}B_{jm}^{(2)}\psi_{im}\right)=0$$
$$RhK_3(x,\theta)\left(\varphi_{ij}+\frac{1}{R}\sum_{m=1}^{N_\theta}B_{jm}^{(1)}w_{im}\right)-R\frac{h^3}{24}\frac{\partial K_1(x,\theta)}{\partial x}$$
$$\left(\sum_{n=1}^{N_x}A_{in}^{(1)}\varphi_{nj}+\frac{1}{R}\sum_{m=1}^{N_\theta}B_{jm}^{(1)}\psi_{im}\right)-R\frac{h^3}{24}K_3(x,\theta)\left(\sum_{n=1}^{N_x}A_{in}^{(2)}\varphi_{nj}\right.$$
$$\left.+\frac{1}{R}\sum_{m=1}^{N_\theta}A_{in}^{(1)}B_{jm}^{(1)}\psi_{nm}\right)-\frac{h^3}{12}\frac{\partial K_1(x,\theta)}{\partial\theta}\sum_{n=1}^{N_x}A_{in}^{(1)}\psi_{nj}$$
$$-\frac{h^3}{12}K_2(x,\theta)\sum_{n=1}^{N_x}\sum_{m=1}^{N_\theta}A_{in}^{(1)}B_{jm}^{(1)}\psi_{nm}-\frac{h^3}{12R}\frac{\partial K_1(x,\theta)}{\partial\theta}$$
$$\sum_{m=1}^{N_\theta}B_{jm}^{(1)}\varphi_{im}-\frac{h^3}{12R}K_1(x,\theta)\sum_{m=1}^{N_\theta}B_{jm}^{(2)}\varphi_{im}=0 \qquad (26)$$

The Chebyshev – Gauss – Lobatto distribution is assumed, for which the coordinates of grid points along the reference surface are [33, 34]

$$x_i=\frac{L}{2}\left(1-cos\frac{(i-1)\pi}{N_x-1}\right)\qquad for\ \ i=1,2,\dots,N_x$$
$$\theta_j=\frac{\alpha}{2}\left(1-cos\frac{(j-1)\pi}{N_\theta-1}\right)\qquad for\ \ j=1,2,\dots,N_\theta \qquad (27)$$

The Chebyshev–Gauss–Lobatto sampling points rule guarantees convergence and efficiency to the GDQ technique. To carry out the analysis and obtain critical temperature difference using eigenvalue method and GDQM, in the calculations, the domain and the boundary degrees of freedom are separated, and in vector forms they are denoted as (d) and (b), respectively. Based on this definition, equations can write as follow [33]

$$\{x_d\}=\{\{u_d\},\{v_d\},\{w_d\},\{\psi_d\},\{\varphi_d\}\}$$
$$\{x_b\}=\{\{u_b\},\{v_b\},\{w_b\},\{\psi_b\},\{\varphi_b\}\} \qquad (28)$$

Introducing Eqs. (27) and (28) to Eq. (26), stability equations and the boundary conditions are as follow

$$[A_{db}]\{X_b\}+[A_{dd}]\{X_d\}=0$$
$$[A_{bb}]\{X_b\}+[A_{bd}]\{X_d\}=0 \qquad (29)$$

Where simplified as follow

$$\begin{bmatrix}[A_{bb}] & [A_{bd}]\\ [A_{db}] & [A_{dd}]\end{bmatrix}\begin{Bmatrix}\{X_b\}\\ \{X_d\}\end{Bmatrix}=0 \qquad (30)$$

4. Results and discussion

In order to obtain the critical temperature difference for a piezo-magnetic two dimensional functionally graded materials (2D-PFGM) cylindrical panel subjected to magnetic field with simply supported boundary conditions (SSSS), GDQM was used in conjunction with a program being written in MATLAB. The 2D FGM cylindrical panel made of two metals and two ceramics include Nickel (Ni), stainless Steel, Silicon Nitride and Alumina whose material properties are given in Table 1 [34, 35]. To study the influence of uniform magnetic field on critical temperature buckling of the cylindrical panel, Cobalt Ferrite piezomagnetic fibers are distributed uniformly in longitudinal direction (x) through the FG matrix. Material properties of Cobalt Ferrite are given in Table 2.

Table 1: Material properties of Constituents of the 2D-FGM cylindrical panel.

Constituents	Material	E (GPa)	α(1/℃)
m1	Ni	204	13.2e-6
m2	Stainless steel	207.79	15.32e-6
c1	Silicon nitride	322.27	7.4746e-6
c2	Alumina	380	7.4e-6

Table 2: modulus of Piezomagnetic.

Piezomagnetic	Piezomagnetic constant (N/Am)
Cobalt Ferrite	$q_{31}=q_{32}=580.3$, $q_{33}=699.7$, $q_{24}=q_{15}=550$

In order to demonstrate the accuracy of the present analysis, some illustrative examples are solved and the numerical results are compared with the data available in open literature. The comparison of critical temperature difference ΔT_{cr} for the simply supported isotropic cylindrical panels with results reported in reference [13], are tabulated in Table 3. In this analysis, four different cylindrical shells made of various isotropic materials are considered whose material properties are given in Table 1. The geometrical parameters of cylindrical shells are: $L/R=0.8$, $\alpha=360°$. It can be observed from Table 3 that the present

results agreed well with results reported in reference [13].

Table 3: The convergence of the critical temperature difference of 2D-FG cylindrical shell.

Number of nodes	ΔT_{cr}
7*7	183.2926
9*9	101.12
11*11	102.8108
13*13	100.5093
15*15	100.5093
17*17	100.142

Table 4: Comparison of the critical temperature difference of open cylindrical shell ($L/R = 0.8, \alpha = 360°$).

Materials	h/R	present	Ref. [8]
Ni	0.008	256.8651	256.96
	0.02	638.8089	642.42
	0.05	1564.40	1606. 60
Stainless steel	0.008	221.3198	221.409
	0.02	550.4089	553.524
	0.05	1348.001	1383.81
Silicon nitride	0.008	453.6189	453.803
	0.02	1128.10	1134.508
	0.05	2762.80	2836.27
Alumina	0.008	458.1918	458.3783
	0.02	1139.50	1145.945
	0.05	2790.60	2864.864

In Figs. 4 the effects of variation of central angle α of the cylindrical panel on critical temperature difference of the cylindrical panel for various values of external surface magnetic voltage V_H is presented. The geometrical and material properties of 2D-PFGM cylindrical panel are as follow: $h/R = 0.02, L/R = 0.8, n_\theta = 1, n_x = 4$ and V_H = -300A, 0, 300A. It can be observed from Figs. 4 for $\alpha \leq 70°$ the variation of critical temperature difference of the panel is regular and the increase of α yields decrease of the critical temperature difference ΔT_{cr}, for $\alpha \geq 70°$, as α increase ΔT_{cr} is reduced. Also for $\alpha \geq 70°$, increase of surface magnetic voltage V_H leads to increasing the critical temperature difference ΔT_{cr}. Moreover, the slope of the curves for $\alpha \geq 190°$ reduced, i.e. the variation of ΔT_{cr} versus α is not very significant.

Effect of the external surface magnetic voltage on the critical temperature difference of the 2D-PFGM cylindrical panel, for various values of thickness to radius ratio *h/R*, is depicted in Fig. 5. In this analysis geometrical and material properties of panel are: $\alpha = 100^\circ, L/R = 0.8, n_\theta = 1, n_x = 3$. Results of Fig. 8 reveal variations of external surface magnetic voltage V_H have minor effects on the critical temperature difference ΔT_{cr}.

5. Conclusion

In this paper, Magneto-Thermo-Elastic buckling analysis of a 2D PFGM open cylindrical shell subjected to magnetic field based on first order shear deformation theory is investigated. The constituent volume fraction is estimated through a volume fraction power-law. The material properties of the 2D FGM shell are assumed to vary through the longitudinal and circumferential directions according to a linear rule of mixtures. The nonlinear strain-displacement relations in cylindrical coordinates is considered. Total potential energy function for magneto-thermo-elastic loading is written. The variation method is applied to the total potential energy, and nonlinear stability equations of open shells are obtained. These equations are discretized by means of the generalized differential quadrature method (GDQM) to obtain critical temperature difference. Results are presented on the effect of applied voltage to the external surface of panel, and the central angle of the panel. Numerical comparisons is done by the result of an open literature for showing validity of the study. Good agreements show the accuracy of the present study.

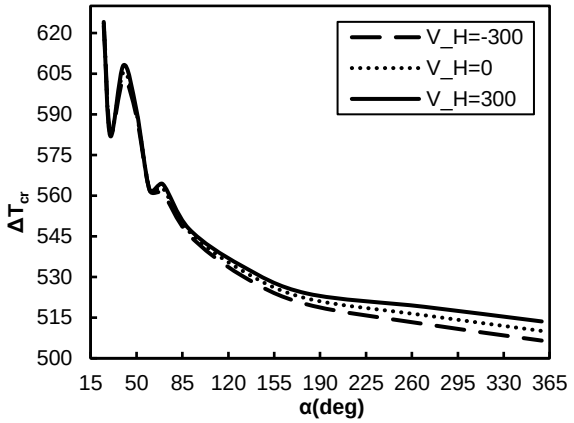

Fig. 4: Effect of central angel of the cylindrical panel on the critical buckling temperature.
($h/R = 0.02, L/R = 0.8, n_\theta = 1, n_x = 4$)

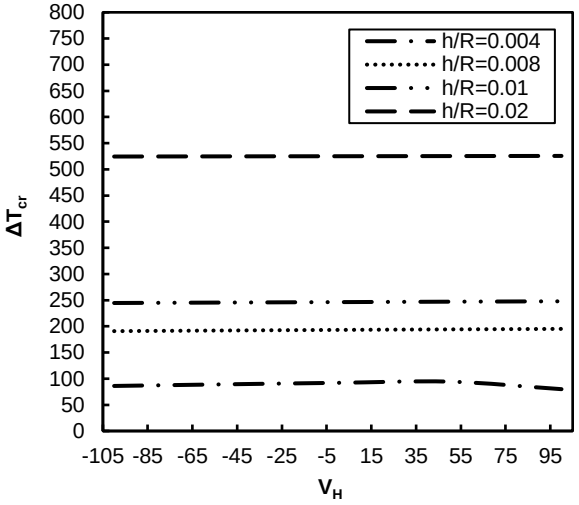

Fig. 8: Effect of external surface magnetic voltage V_H on the critical buckling temperature of the cylindrical panel for different value of *h/R* ($\alpha = 100^\circ, L/R = 0.8, n_\theta = 1, n_x = 3$)

6. References

[1] Koizumi M. The concept of FGM, Ceramics Transactions, Functionally Gradient Materials 1993; 34:3-10.

[2] Li JY. Magneto-electro-elastic multi-inclusion and inhomogeneity problems and their applications in composite materials. International Journal of Engineering Science 2000; 38:1993-2011.

[3] Huang JH, Kuo WS. The analysis of piezoelectric/piezomagnetic composite materials containing ellipsoidal inclusions. Journal of Applied Physics 1997; 81(3): 1378-1386.

[4] Li JY, Dunn ML. Anisotropic coupled-field inclusion and inhomogeneity problems. Ph Magazine A, 1998; 77(5):1341-1350.

[5] J. Y. Li, M. L. Dunn, "Analysis of microstructural fields in heterogeneous piezoelectric solids", International Journal of Engineering Science 1999; 37: 665-685.

[6] Pan E. Exact solution for simply supported and multilayered magneto-electro-elastic plates. J. Appl. Mech., ASME; 200168:608–618.

[7] Pan E, Heyliger PR. Free vibrations of simply supported and multilayered magneto-electro-elastic plates. Journal of Sound and Vibration 2002;252:429–442.

[8] Bhangale RK, Ganesan N. Static analysis of simply supported functionally graded and layered magneto-electro-elastic plates. International journal of solids and structures 2006; 43(10):3230–53.

[9] Shen H. Postbuckling of nanotube-reinforced composite cylindrical shells in thermal enviroments. PartI:Axially load shells. Composite Structures 2011;93:2096-2108.

[10] Shen H. Postbuckling of nanotube-reinforced composite cylindrical shells in thermal enviroments. PartII:Pressure load shells, Composite Structures 2011;93:2496-2503.

[11] Darvizeh M, Darvizeh A, Ansari R. Thermal Buckling Analysis of Mderately Thick Composite cylindrical shells under Axiymmetric Thermal loading. Mech and Aerospace Eng 2007;3(2):99-107.

[12] Shariyat M. Dynamic thermal buckling of suddenly leated temperature dependent FGM cylindrical shells under combined axial compression and external pressure. International Journal of Solids and Structures 2008;45:2598-2613.

[13] Eslami MR, Ziaii AR, Ghorbanpour A. Thermoelastic buckling of thin cylindrical shells based on improved stability equations. Journal of Thermal Stresses 1996;19(4):299-315.

[14] Jabbari M, Dehbani H. An exact solution for classic coupled magneto-thermo-elasticity in cylidrical coordinates. Journal of Solid Mechanics 2012;4(1):33-47.

[15] Long Z, Xuewu L. Buckling and vibration analysis of functionally graded magneto-electro-thermo-elastic circular cylindrical shells, Applied Mathematical Modelling 2013;37:2279-2292.

[16] Aboudi J. Micromechanical Prediction of the Effective Behavior of Fully CoupledElectro-Magneto-Thermo-Elastic Multiphase Composites. Tel Aviv University, Tel Aviv, Israel NASA / CR-2000-209787.

[17] LEE S J. Efective properties of three-phase electro-magneto-elastic multifunctional composite materials. Major Subject: Aerospace Engineering December 2003.

[18] Biju B, Ganesan N, Shankar K. Response of multiphase magneto-electro-elastic sensors under harmonicmechanical loading. International Journal of Engineering,Science and Technology 2009;1(1):216-227.

[19] Tang Tian,Wenbin.Yu. Micromechanical modeling of the multiphysical behavior of smart materials using the variational asymptotic method. Smart Mater. Struct. 2009;18:125026, 14pp.

[20] Kondaiah P, Shankar K,Ganesan N. Pyroelectric and pyromagnetic effects on behavior of magneto-electro-elastic plate. Coupled Systems Mechanics 2013;2(1):1-22.

[21] Malekzadeh P, Heydarpour Y. Response of functionally graded cylindrical shells under moving thermo-mechanical loads. Thin-Wall Structures 2012; 58: 51–66.

[22] Jafari Mehrabadi S, Sobhani Aragh B. On the thermal analysis of 2-D temperature-dependent functionally graded open cylindrical shells. Composite Structures 2013; 96:773–785.

[23] Bellman RE, Casti J. Differential quadratured and long term Integration. Journal of Mathematical Analysis and Applications 1971;34(1):235-238.

[24] Shu C, Du H. Free vibration analysis of laminated composite cylindrical shells by DQM. Compos Technol Part B, 1997;28:267-274.

[25] Shu C, Richards BE. Application of generalized differential quadrature to solve two-dimensional incompressible Navier Stokes equations. Int J Numer Methods Fluids 1992;15:791–8.

[26] Bert CW, Malik M. Differential quadrature method in computational mechanics, a review. Appl Mech Rev 1996;49:1–28.

[27] Tornabene F, Viola E. Vibration analysis of spherical structural elements using the GDQ method. Comput Math Appl 2007;53:1538–60.

[28] Asgari M, Akhlaghi M. Natural frequency analysis of 2-D FGM thick hollow cylinder based on three-dimensional elasticity equtions. European Journal of Mechanics A/Solids, 2011;30:72-81.

[29] Reddy JN. Mechnics of laminated composite plates and shells. Theory and Analysis, CRC Press, Boca Raton, FL, Second edition, 2004.

[30] Wu C, Tsai Y. Static behavior of functionally graded magneto-electro-elastic shells under electric displacement and magnetic flux. International Journal of Engineering science, 2007;45:744-769.

[31] Brush DO, Almorth BO. Buckling of Bars, Plates and Shells. McGraw-Hill, New York, 1975.

[32] Bodaghi M, Shakeri M. An analytical approach for free vibration and transient response of functionally graded piezoelectric cylyndrical panels subjected to impulsive loads. Composite Structures 2012;94:1721-1735.

[33] Shu C. Differential Quadrature and Its Applications in Engineering. springer, Berlin, 2000.

[34] Yang J, Liew K.M, Wu YF. Thermomechanical postbuckling of FGM cylindrical panels with temprature-dependent properties. International journal of solids and structures 2006;43:307-324.

[35] Fu Y, Wang J, Mao Y. Nonlinear analysis of buckling,free vibration and dynamic stability for the piezoelectric FG beams in thermal enviroment. Applied mathematical modeling 2012;36:4324-4340.